Carbohydrate Polymers 157 (2017) 484–492

Contents lists available at ScienceDirect

Carbohydrate Polymers

journal homepage: www.elsevier.com/locate/carbpol

Structural elucidation of three antioxidative polysaccharides from *Tricholoma lobayense*

Yan Chen*[,1], Xue-Hui Li[1], Li-Yuan Zhou, Wan Li, Liu Liu, Dan-Dan Wang, Wen-Na Zhang, Sajid Hussain, Xiao-He Tian, Yong-Ming Lu*

School of Life Sciences and Key Laboratory for Ecological Engineering and Biotechnology, Anhui University, Hefei 230601, PR China

ARTICLE INFO

Article history:
Received 29 July 2016
Received in revised form 5 October 2016
Accepted 5 October 2016
Available online 6 October 2016

Keywords:
Tricholoma lobayense
Polysaccharides
Structural elucidation
Antioxidant activity

ABSTRACT

Tricholoma lobayense is a nutritious mushroom with great health benefits. Three polysaccharides with purity higher than 99% were successfully extracted from *Tricholoma lobayense*. The molecular weights of TLH-1, TLH-2 and TLH-3 were determined to be 8.43×10^5, 5.36×10^5 and 4.53×10^3 Da, respectively. The backbones of TLH-1 and TLH-2 were mainly composed of 1,4-linked α-D-glucopyranosyl. However, polysaccharide TLH-3 was found to be a highly branched glucogalactan, which is made up of 1,3-linked α-D-glucopyranosyl branched at C-6 and 1,3-linked β-D-galactopyranosyl. In vitro antioxidant activity assays revealed that TLH-3 exhibited highest antioxidant activities among the polysaccharides from *Tricholoma lobayense*, which were comparable to those of ascorbic acid. The results suggested that the outstanding antioxidant activities of TLH-3 might depend on its low molecular weight, high branch degree, versatile linkage types and complex conformation. These characteristics make TLH-3 an attractive natural antioxidant for food and pharmaceutical applications.

1. Introduction

Mushrooms, famous edible fungi for their delicacy, have many nutritious and medical values (Chang & Buswell, 1996; Wasser, 2002). Polysaccharides from mushrooms not only play an important role in the growth and development of living organisms but also possess diverse biological properties, including antioxidant, antitumor, antibacterial and immunomodulatory activities (Chang et al., 2015; Giavasis, 2014; Li, Wang, Wang, Walid, & Zhang, 2012; Villares, Mateo-Vivaracho, & Guillamón, 2012; Zhang, Cui, Cheung, & Wang, 2007). Nowadays, the application of polysaccharides as food additives has drawn more and more attentions in food industry (Xu, Xu, & Zhang, 2012). In most cases, functions are closely related to polysaccharides' structural properties, such as linkage type, branch degree, tertiary structure, and molecular weight (Chen, Xiao, Wang, Fang, & Ding, 2012; Wang et al., 2014; Xu, Dong, Cong, & Ding, 2010; Zhu et al., 2013). For example polysaccharide PL-3 from *Ganoderma lucidum* which consists of 1,3-linked β-D-glucopyranosyl units could enhance the proliferation of T-type and B-type lymphocytes in vitro, whereas PL-1 which has a backbone of 1,4-linked α-D-glucopyranosyl and 1,6-linked β-D-galactopyranosyl exhibits an immune-stimulating activity in mice (Bao, Wang, Dong, Fang, & Li, 2002). 1,3-β-D-Glucan from *Ganoderma lucidum* possesses an excellent antioxidant capability against H_2O_2-induced cell death by attenuating intracellular ROS and inhibiting SMase activity, which might be attributed to its low molecular weight. (Kao et al., 2012).

Tricholoma lobayense is a nutritious and precious edible mushroom, which was discovered in Africa and named by French mycologists in 1970. The unique flavor, taste and health-beneficial effect make it popular among Africa and Asia (Weng et al., 2013). Previously, three polysaccharides (TLH-1, TLH-2 and TLH-3) were successfully isolated from the fruiting bodies of *Tricholoma lobayense* in our lab (Liu, Lu, et al., 2015). Antioxidant activity studies revealed that polysaccharide TLH-3 could scavenge superoxide radicals in vitro much more effectively than TLH-1 and TLH-2. Furthermore, the scavenging capacity of TLH-3 was comparable to that of ascorbic acid (Wang et al., 2012), a commercially available antioxidant. However, the origin of this excellent antioxidant activity is not known yet.

In order to demonstrate the reason responsible for the antioxidant activities of the three polysaccharides from *Tricholoma lobayense*, high performance liquid chromatography (HPLC), methylation analysis, 1D (^{1}H, ^{13}C) and 2D (COSY, HMQC and HMBC)

* Corresponding authors.
E-mail addresses: chenyan91030@yahoo.com (Y. Chen), ymlu@ahu.edu.cn (Y.-M. Lu).
[1] These authors contributed equally to this work.

http://dx.doi.org/10.1016/j.carbpol.2016.10.011
0144-8617/

NMR spectroscopy were used for the structure characterization. Structure features including physicochemical properties, monosaccharide composition, glycosidic bonds and chain conformations were elucidated. Furthermore, antioxidant activities were examined by DPPH, superoxide, hydroxyl and ABTS radicals scavenging assays. The results were analyzed and compared to clarify the structure-activity relationship.

2. Materials and methods

2.1. Materials and reagents

Tricholoma lobayense was purchased from Panji Shenshan edible fungus cooperative (Huainan, Anhui Province, China). Crude polysaccharides were extracted from *Tricholoma lobayense* by high-pressure homogenization. Polysaccharide TLH-1, TLH-2 and TLH-3 used in this study were obtained by precipitation with 60% ethanol and ultrafiltration according to the method of Liu, Lu, et al., (2015) with some modifications. Deuterium oxide (D_2O) was purchased from Sigma Chemical Co. (St. Louis, MO, USA). Seven monosaccharide standards (Rhamnose 99%, Mannose 99%, Glucuronic acid 98%, Galacturonic acid 97%, Glucose 99.5%, Galactose 99%, Arabinose 98%) were purchased from Aladdin Industrial Corporation. All other chemicals and solvents used in this study were of analytical grade.

2.2. Physical and chemical properties analysis

The purity and molecular weights of three polysaccharides were determined by HPLC on an Agilent 1260 system (Agilent Technologies, Palo Alto, CA, USA) equipped with an evaporative light scattering detector (ELSD) and a TSK gel G4000 PWXL column (300 × 7.8 mm, Tosoh Corp, Tokyo, Japan). The linear regression was calibrated with T-series dextran standards (T-3, T-10, T-40, T-100, T-200, T-500 and T-1000). Sample solution (2 mg/mL, 10 μL) was injected and eluted with distilled water at 30 °C with a flow rate of 1.0 mL/min.

Content of the total sugars, proteins and uronic acids in the three purified fractions were determined colorimetrically using phenol-sulfuric acid (Masuko et al., 2005), Bradford method (Bradford, 1976) and meta-hydroxydiphenyl-sulfuric acid (Blumenkrantz & Asboe-Hansen, 1973), respectively. The IR spectra of the polysaccharides were determined using Fourier Transform IR Spectrophotometry (FT-IR, Nicolet 380, Thermo, USA). The purified polysaccharides (1 mg) were ground with KBr powder (100 mg) and then pressed into pellets for FT-IR measurement in the frequency range of 4000–400 cm^{-1}.

2.3. Monosaccharide composition analysis

Each polysaccharide (10 mg) was hydrolyzed by trifluoroacetic acid (TFA, 2 mol/L), followed by complexing with 1-phenyl-3-methyl-5-pyrazolone (PMP) (0.5 mol/L). The resulting products were then analyzed by HPLC equipped with a ZORBAX Eclipse XDB-C18 column (150 × 4.6 mm, particle size 5 μm, Agilent Technologies, CA, USA) and a UV detection at 245 nm. Sample solution (10 μL) was injected and eluted with distilled water at 25 °C with a flow rate of 1.0 mL/min. The mobile phase A was a mixture of phosphate buffer (50 mmol/L)-acetonitrile (85:15, v/v) and the mobile phase B was a mixture of phosphate buffer (50 mmol/L)-acetonitrile (60:40, v/v). The analysis was carried out with a gradient elution of 15-23-15% phase B from 0 to 20–35 min.

2.4. Methylation and GC–MS analysis

The sample (20 mg) was methylated with methyl iodide three times (Liu & Sun, 2011; Yan, Yin, Zhang, Yang, & Yu, 2013). Then partially methylated products were hydrolyzed with TFA for 6 h at 100 °C, followed by reduction with $NaBH_4$ and acetylation with acetic anhydride. The partially methylated alditol acetates were analyzed by GC–MS (Agilent 7890A/5975C, USA) equipped with a HP-5 capillary column (30 m × 0.32 mm, 0.50 μm, Agilent Technologies, CA, USA) programmed from 120 (keep for 1 min) to 240 °C (keep for 6.5 min) at 10 °C per min. The degree of branching (DB) could be calculated with the following equation (Wu et al., 2014):

$$DB = \frac{NT + NB}{NT + NB + NL} \quad (1)$$

where NT, NB and NL are the total contents of the terminal residues, branched residues, and backbone residues, respectively.

2.5. NMR analysis

The NMR spectra of TLH-1, TLH-2 and TLH-3 were obtained by an AVANCE-600 NMR spectrometer (Bruker Inc., Rheinstetten, Germany). 40 mg of the dried sample was dissolved in deuterium oxide (D_2O, 0.5 mL) at room temperature for 3 h before NMR analysis. The ^1H (600Mz) and ^{13}C (150Mz) NMR spectra were recorded at 50 °C. Then, the 2D NMR spectra including $^1H/^1H$ correlation experiments (COSY), Heteronuclear Multiple-Quantum Coherence (HMQC) and Heteronuclear Multiple Bond Correlation (HMBC) were recorded.

2.6. In vitro antioxidant activities analysis

2.6.1. DPPH radical scavenging activity

Two milliliters of aqueous solution of TLH-1, TLH-2 and TLH-3 (50, 100, 200, 300, 400 and 500 μg/mL) were mixed with DPPH-methanol solution (2 mL, 0.13 mM). The mixture was shaken vigorously and left to stand in test tubes covered in aluminum foil for 30 min at 25 °C. Then the absorbance at 517 nm was measured (Jing et al., 2015). Ascorbic acid was used as positive control. The DPPH radical scavenging activity (RSA) was calculated according to the following equation:

$$\text{DPPH RSA}(\%) = \left(1 - \frac{A_2 - A_1}{A_0}\right) \times 100 \quad (2)$$

where A_0 is the absorbance value of DPPH-methanol solution (2 mL) plus methanol (2 mL). A_1 is the absorbance value of the mixture of methanol (2 mL) plus samples (2 mL) with different concentrations. A_2 is the absorbance value of DPPH-methanol solution (2 mL) plus samples (2 mL) with different concentrations. All assays were carried out in triplicate.

2.6.2. Superoxide radical scavenging activity

0.5 mL of phosphate buffer (50 mM, pH 8.3) and 0.4 mL of aqueous samples (50, 100, 200, 300, 400 and 500 μg/mL) were mixed and stored for 20 min at 25 °C. Then 0.1 mL of pyrogallol (3 mM) preheated to 25 °C was added. The absorbance value of the mixture was measured at 325 nm every 30 s for 5 min (Zhu & Wu, 2009). Ascorbic acid was used as positive control. Superoxide RSA was calculated according to the following equation:

$$\text{Superoxide anion RSA}(\%) = \frac{\Delta A_2 - \Delta A_1}{\Delta A_0} \times 100 \quad (3)$$

where ΔA_1 is the difference of absorbance value per 30 s for different concentrations of samples. ΔA_0 is the difference of absorbance value per 30 s without samples. All assays were carried out in triplicate.

2.6.3. Hydroxyl radical scavenging activity

Mixtures containing 1 mL of $FeSO_4$ (6 mM), 1 mL of ethanol-salicylic acid (6 mM) and 1 mL of aqueous sample (50, 100, 200, 300, 400 and 500 μg/mL) were incubated in test tubes, shaken and left to stand for 10 min. Then, 1 mL of H_2O_2 (2.4 mM) was added and the test tubes were covered in aluminum foil. After storing at 37 °C for 30 min, the presence of hydroxyl radical was detected by monitoring the absorbance at 510 nm. Ascorbic acid was used as positive control. Hydroxyl RSA was calculated by the following equation:

$$\text{Hydroxyl}\quad \text{RSA}(\%) = \left(1 - \frac{A_2 - A_1}{A_0}\right) \times 100 \tag{4}$$

where A_0 is the absorbance value of the solution without the samples. A_2 is the absorbance value of the samples solution with different concentrations. A_1 is the absorbance value of the solution without ethanol-salicylic acid.

2.6.4. Total antioxidant capacity

After reacting aqueous ABTS (2, 2′-Azinobis-(3-ethylbenzthiazoline-6-sulphonate)) solution with potassium persulfate (2.45 mM) at room temperature for 14 h, ABTS radical cation ($ABTS^{\bullet+}$) was obtained according to the literature (Barahona, Chandía, Encinas, Matsuhiro, & Zúñiga, 2011). The $ABTS^{\bullet+}$ solution was diluted with PBS (pH 7.0) until the absorbance at 734 nm was 0.70. Then 10 μL of polysaccharide samples (50, 100, 200, 300, 400 and 500 μg/mL) in PBS was mixed with 200 μL of the diluted $ABTS^{\bullet+}$ solution and the absorbance value was measured at 734 nm. Ascorbic acid was used as positive control. ABTS RSA was calculated by the following equation:

$$\text{ABTS}\quad \text{RSA}(\%) = \left(1 - \frac{A_j - A_i}{A_0}\right) \times 100 \tag{5}$$

where A_0 is the absorbance value of the $ABTS^{\bullet+}$ solution with 10 μL of PBS. A_j is the absorbance value of the $ABTS^{\bullet+}$ solution in presence of samples with different concentrations. A_i is the absorbance value of the samples solution in the absence of $ABTS^{\bullet+}$.

2.7. Statistical analysis

The data were mean ± standard deviation (SD) of three replicates except for cell tests of four replicates. Statistical significance was determined by the one-way analysis of variance (ANOVA), and P value less than 0.05 was considered statistically significant.

3. Results

3.1. Antioxidant activities of TLH-1, TLH-2 and TLH-3

The antioxidant activities of TLH-1, TLH-2 and TLH-3 were presented in Fig. 1 and IC_{50} values were listed in Table S1. Four assays were used to evaluate the antioxidant capacities of the three polysaccharides. The results indicated that with increasing concentration of polysaccharides, the scavenging activities towards DPPH, superoxide, hydroxyl and ABTS radicals were also enhanced. The scavenging abilities of TLH-1 and TLH-2 were similar, but those of TLH-3 were much higher and similar to those of ascorbic acid.

3.2. Physical and chemical properties of TLH-1, TLH-2 and TLH-3

The content of total saccharides of TLH-1, TLH-2 and TLH-3 were 99.7%, 99.6% and 99.3%, respectively. The content of uronic acids for TLH-1, TLH-2 and TLH-3 were 0, 3.01% and 6.44%, respectively. As shown in Fig. S1a-c, only one symmetrical sharp peak was found, which indicated that all the obtained polysaccharides were homogeneous. According to the calibration curve of standards ($\log M_W = -0.350t + 7.449$, $R^2 = 0.997$), the molecular weights of TLH-1, TLH-2 and TLH-3 were calculated to be 8.43×10^5, 5.36×10^5 and 4.53×10^3 Da, respectively.

Fourier transform infrared spectroscopy has been broadly used for the characterization of polysaccharides. The FT-IR spectra of TLH-1, TLH-2 and TLH-3 were depicted in Fig. S1d. Five typical signals were clearly presented at nearly 3394, 2931, 1643, 1413 and 1037 cm^{-1} for all the three polysaccharides, which could be assigned for the stretching vibration of O—H and C—H, the bending vibration of O—H and C—H, and a pyranose form of sugars, respectively. The bands at about 850 cm^{-1} and 890 cm^{-1} for the three polysaccharides suggested a α configuration and a β anomeric configuration (Calonje, García Mendoza, & Novaes-Ledieu, 1996; Wang, Zhang, Zhang, & Chen, 2008). These results indicated that all the three components were polysaccharides.

3.3. Monosaccharide composition of TLH-1, TLH-2 and TLH-3

As shown in Fig. 2, fraction TLH-1 was composed of rhamnose, mannose, glucose, galactose and arabinose with the molar ratio of 0.02: 1.00: 3.22: 0.01: 0.28, which could be denoted as a glucan. However, fraction TLH-2 and TLH-3 were made up of rhamnose, mannose, glucuronic acid, galacturonic acid, glucose, galactose and arabinose, while the molar ratio was 0.02: 1.00: 0.05: 0.04: 3.80: 0.03: 0.28 and 0.47: 1.00: 0.13: 0.10: 9.84: 6.18: 0.93, respectively. The monosaccharide composition of TLH-2 was similar to TLH-3, whereas the molar ratio of monosaccharide was very close to TLH-1. Thus TLH-2 could also be mainly regarded as a glucan. In contrast TLH-3, made up of seven monosaccharides with higher molar ratio than TLH-2, could be noted as a glucogalactan (Liu, Wen, Kan, & Jin, 2015; Zhu, Han, Sun, Wang, & Yang, 2012).

3.4. Linkage types of TLH-1, TLH-2 and TLH-3

To determine the linkage types, TLH-1, TLH-2 and TLH-3 were methylated and converted into the corresponding alditol acetates for further GC–MS analysis. As shown in Table 1 and Fig. S2, the major derivative from TLH-1 and TLH-2 was both 2, 3, 6-tri-O-methyl glucitolpyranosyl with a molar ratio of 38.96 and 26.54, respectively. The DB values of TLH-1 and TLH-2 were calculated to be 0.27 and 0.23, implying they were both small-branched polysaccharides. However, the major derivatives from TLH-3 were composed of 2, 4-Me_2-Glc*p*, 2,3,4,6-Me_4-Glc*p*, 2,3,6-Me_3-Glc*p*, and 2,4,6-Me_3-Gal*p*. The DB value of TLH-3 was 0.74, suggesting a highly-branched structure. These results were substantially consistent with the results of monosaccharide composition analysis mentioned above.

3.5. NMR study of TLH-1

Four dominant peaks were found at δ 5.37, 5.08, 5.05 and 4.99 ppm in the anomeric region of ^1H NMR spectrum of TLH-1 (Fig. S3a), indicating that these glucosyl residues were α-glycosidically linked except the residue presented at δ 4.99 ppm. The chemical shift of H-2 can be assigned from the COSY spectrum based on the principle that H-2 correlates with H-1 (Fig. S3b). Other hydrogen signals (H-3 to H-6) were also assigned by the same analogy. The corresponding anomeric carbons were identified from cross peaks in the HMQC spectrum at δ 102.06, 101.11, 104.15 and 100.54 ppm (Fig. S3c). All the ^1H and ^{13}C chemical shifts for TLH-1 were listed in Table 2. According to literature data (Cao et al., 2006; Chen, Zhang, Chen, & Cheung, 2014; Chen et al., 2011; Golovchenko, Khramova, Ovodova, Shashkov, & Ovodov, 2012; Kang et al., 2011; Yin et al., 2010), these cross peaks were assigned to 1,4-linked α-D-Glc*p* (A), T-α-L-*Rha*p (D), 1,3,6-linked α-D-Man*p* (C) and T-β-D-Glc*p* (B),

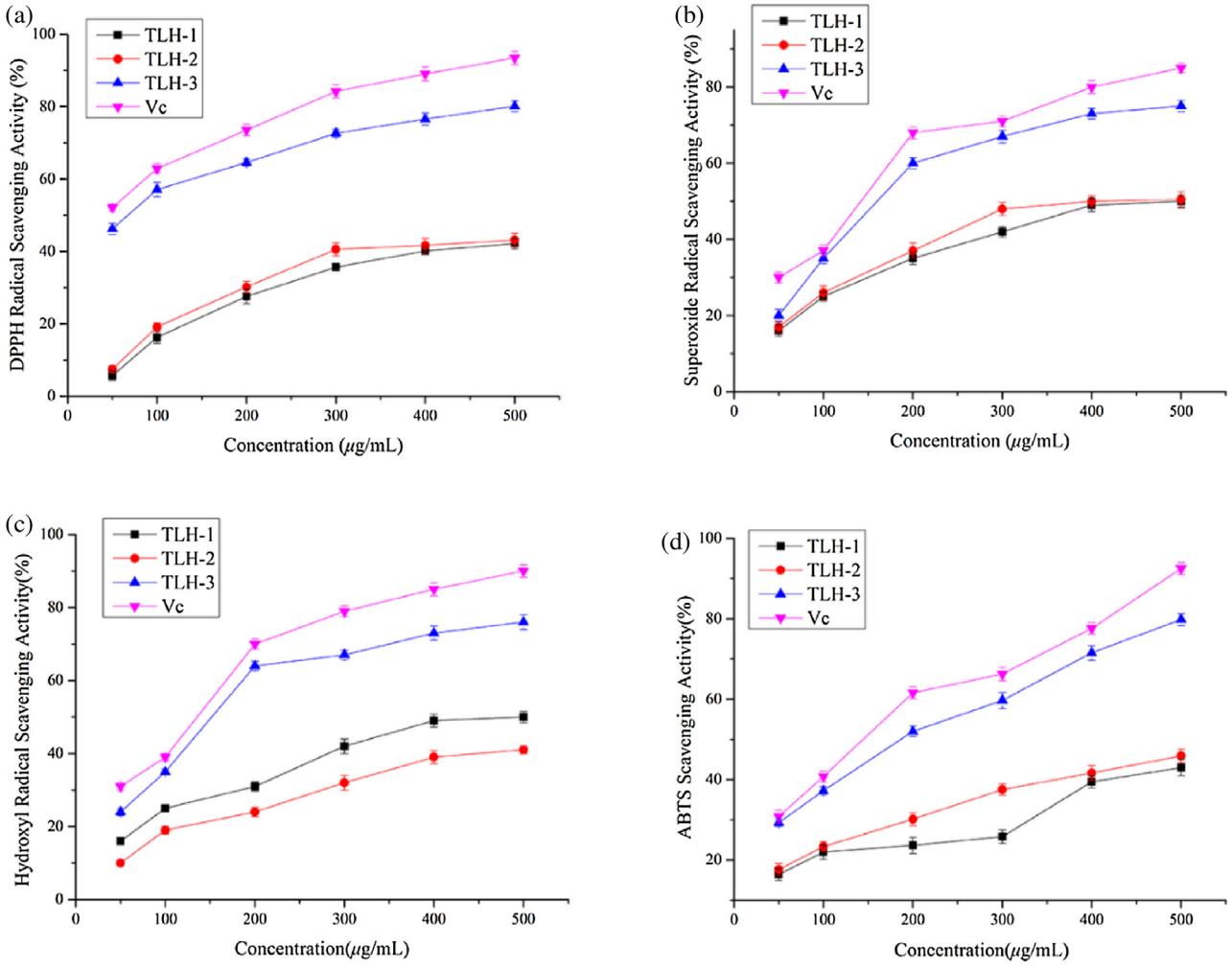

Fig. 1. Scavenging effects of TLH-1, TLH-2, TLH-3 and Vc at different concentrations on DPPH radicals (a), superoxide radicals (b), hydroxyl radicals (c) and ABTS radicals (d). Each value represents the mean ± standard deviation (SD) (n = 3). Vc stands for ascorbic acid as positive control.

Table 1
GC–MS analysis of methylated TLH-1, TLH-2 and TLH-3.

Peak No.	Saccharide derivative	Deduced linkage	Molar ratio		
			TLH-1	TLH-2	TLH-3
1	2,3,5-Me_3-Araf	T-Ara*f*-(1→	1.14	0.83	0.76
2	2, 4-Me_2-Glc*p*	→3,6)-Glc*p*-(1→	1.11	0.99	8.53
3	2,3,6- Me_3-Glc*p*	→4)-Glc*p*-(1→	38.96	26.54	3.08
4	2,3,4,6-Me_4-Glc*p*	T-Glc*p*-(1→	5.83	4.08	4.84
5	2,4,6-Me_3-Gal*p*	→3)-Gal*p*-(1→	0.93	0.58	2.85
6	2,4- Me_2-Man*p*	→3,6)-Man*p*-(1→	5.17	2.61	1.58
7	2,4,6-Me_2-Man*p*	→3)-Man*p*-(1→	1.00	1.00	ND
8	2,3,4,6-Me_4-Rha*p*	T-Rha*p*(1→	1.56	ND	1.00
9	3,4- Me_2-Rha*p*	→2)-Rha*p*(1→	ND	0.32	ND

T: Terminal. ND: Not detected.

Table 2
Summary of ^1H and ^{13}C Chemical Shifts for TLH-1.

	Glycosidic linkage	H1/C1	H2/C2	H3/C3	H4/C4	H5/C5	H6, H'6/C6
A	→4)-α-D-Glc*p*-(1→	5.37	3.59	3.72	3.86	3.91	3.75, 3.89
		102.06	74.36	71.25	75.12	69.13	62.87
B	T-*β*-D-Glc*p*-(1→	4.99	3.84	3.63	3.99	3.74	3.81, 3.92
		100.54	74.78	74.17	71.61	75.22	63.02
C	→3,6)-α-D-Man*p*-(1→	5.05	3.64	3.67	3.79	3.52	3.92
		104.15	65.26	69.13	70.90	74.24	73.55
D	T-α-L-*R*ha*p*-(1→	5.08	4.12	3.92	3.74	3.80	1.35
		101.11	71.24	70.61	72.89	69.01	18.19

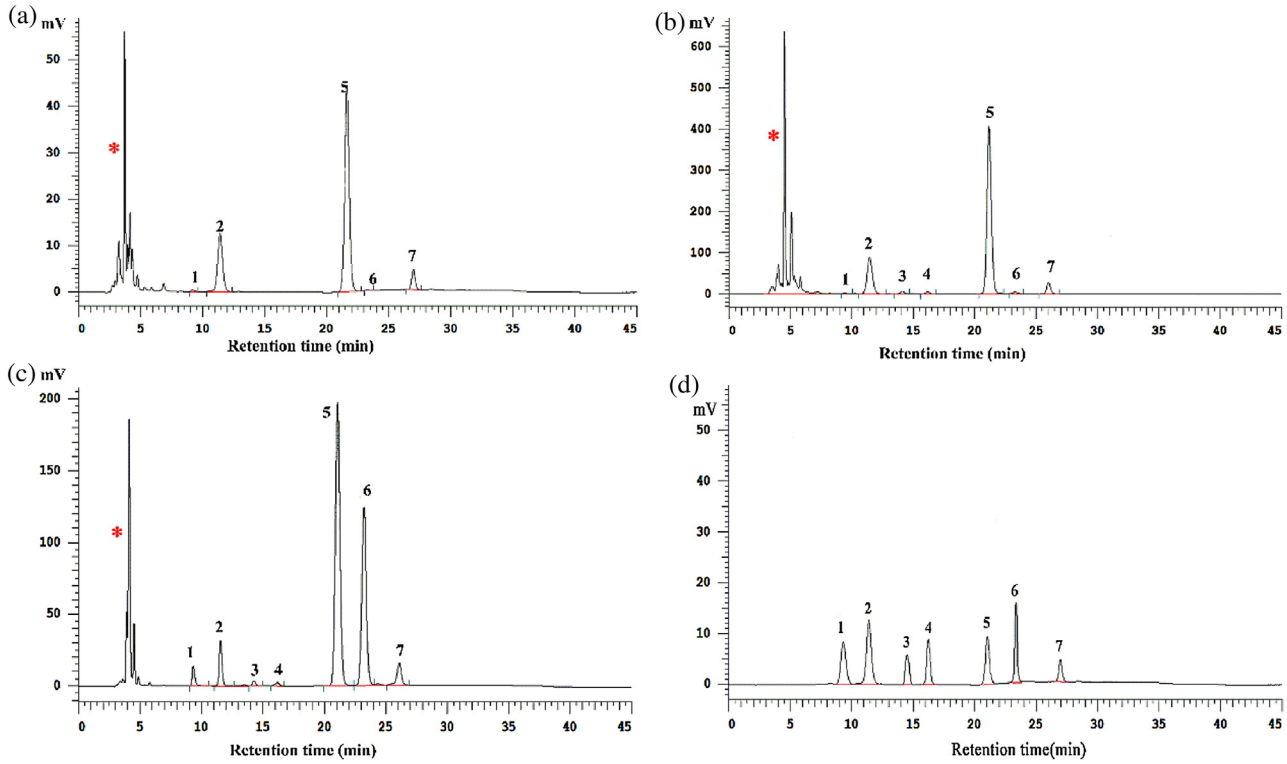

Fig. 2. Chromatograms of monosaccharide compositions of TLH-1 (a), TLH-2 (b), TLH-3 (c) and seven monosaccharide standards (d) (The asterisk indicates solvent peak. 1-rhamnose, 2-mannose, 3-glucuronic acid, 4-galacturonic acid, 5-glucose, 6-galactose, and 7-arabinose).

respectively. However, the signals of sugar residues such as arabinose and galactose were not clearly detected in the NMR spectrum of TLH-1, which was probably due to the low contents of these residues. No typical signal was observed for uronic acid, which was in agreement with the results of meta-hydroxydiphenyl-sulfuric acid treatment.

HMBC experiment was carried out to confirm the sequence of glucosyl residues in the polysaccharide. The HMBC spectrum (Fig. S3d) indicated that the H-1 signals of 1,4-linked α-D-Glc*p* correlated with C-4 of 1,4-linked α-D-Glc*p* and C-6 of 1,3,6-linked α-D-Man*p*. It was also observed that H-1 of 1,3,6-linked α-D-Man*p* correlated with its C-3 and C-6. H-1 of T-α-L-*Rha*p and T-β-D-Glc*p* correlated with C-3 of 1,3,6-linked α-D-Man*p*. Reversely, the cross peak of C-1 of 1,4-linked α-D-Glc*p* correlated with H-4 of 1,4-linked α-D-Glc*p* and so on.

3.6. NMR study of TLH-2

All the ^{1}H and ^{13}C chemical shifts for TLH-2 were listed in Table 3. Three dominant peaks were found at δ 5.24/102.06, 4.91/104.15 and 4.84/100.54 ppm in the anomeric region of the HMQC spectrum of TLH-2 (Fig. S4d). These peaks could be assigned to 1,4-linked α-D-Glc*p* (A), 1,3,6-linked β-D-Man*p* (Cí) and T-β-D-Glc*p* (B), respectively (Cao et al., 2006; Chen et al., 2011, 2014; Golovchenko et al., 2012; Kang et al., 2011; Yin et al., 2010). Due to the low content of rhamnose, arabinose, and galactose, the signals of these residues were not detected. The cross peaks of H-1 to C-6 were clearly observed in the HMBC spectrum (Fig. S4e). The results indicated that the H-1 signals of 1,4-linked α-D-Glc*p* correlated with the C-4 of 1,4-linked α-D-Glc*p* and C-6 position of 1,3,6-linked β-D-Man*p*. H-1 of 1,3,6-linked β-D-Man*p* and T-β-D-Glc*p* correlated with the C-3 of 1,3,6-linked β-D-Man*p*. Reversely, the cross peak of C-1 of 1,4-linked α-D-Glc*p* correlated with the H-4 of 1,4-linked α-D-Glc*p* and so on.

3.7. NMR study of TLH-3

As shown in Fig. S5a-d, TLH-3 also contains 1,4-linked α-D-Glc*p* (A), T-β-D-Glc*p* (B) and 1,3,6-linked β-D-Man*p* (Cí). The chemical shifts of these residues were identical to those of TLH-1 and TLH-2. A dominant peak at δ 4.92/101.11 ppm was observed in the anomeric region of the HMQC spectrum of TLH-3. Signals of H-2, H-3, H-4, H-5 and H-6 of this residue can be assigned at δ 4.10, 3.80, 3.61, 3.77 and 1.75 ppm. According to literature data, this residue can be identified as T-β-L-*Rha*p (Dí). In the ^{1}HNMR spectrum (Fig. S5a), the anomeric hydrogen signal at δ 5.07 ppm should be assigned to α-glycosidically linked residue. The corresponding carbon signal can be confirmed by the HMQC spectrum (Fig. S5d) to be at δ 94.45 ppm in ^{13}C NMR spectrum (Fig. S5b). According to the results of methylation analysis and literature data, this residue can be identified as 1,3,6-linked α-D-Glc*p* (E). From the COSY spectrum (Fig. S5c), H-2 can be assigned at δ 3.38 ppm which correlated with H-1. H-3, H-4, H-5, and H-6 can be assigned to the shifts at δ 3.55, 3.41, 3.86 and 3.45 ppm. The corresponding chemical shifts for carbons of 1,3,6-linked α-D-Glc*p* can be assigned from the HMQC spectrum (Fig. S5d) and the results were listed in Table 4. The assignments were consistent with the literature data (Das et al., 2009; L. Habibi, Heyraud, Mahrouz, & Vignon, 2004; Jing et al., 2014; Sun et al., 2012; Wu et al., 2014; Xu et al., 2010; Yan et al., 2013; Zhao, Kan, Li, & Chen, 2005; Zhu et al., 2013).

As shown in Fig. S5d, the H-1/C-1 signal at δ 4.37/104.51 ppm can be assigned to 1,3-linked β-D-Gal*p* (F), which was consistent with literature data (Golovchenko et al., 2012; Kang et al., 2011; Liu, Lu, et al., 2015; Yin et al., 2010). The assignment of H-2 (δ 3.28 ppm) could be confirmed by its correlation with H-1 in the COSY spectrum (Fig. S5c). The chemical shift of H-3 can be found at δ 3.42 ppm by its correlation with H-2. Accordingly, the chemical shifts of H-4, H-5 and H-6 can also be found at δ 3.93, 3.75, and 3.86 ppm, respectively. The results were listed in Table 4 and completely consistent

Table 3
Summary of ^{1}H and ^{13}C Chemical Shifts for TLH-2.

	Glycosidic linkage	H1/C1	H2/C2	H3/C3	H4/C4	H5/C5	H6, H'6/C6
A	→4)-α-D-Glc*p*-(1→	5.24	3.46	3.80	3.7375.12	3.78	3.60, 3.71
		102.06	74.36	71.25		69.13	62.44
B	T-*β*-D-Glc*p*-(1→	4.84	3.67	3.46	4.0271.61	3.57	3.40, 3.49
		100.54	74.78	74.17		75.22	64.42
Cí	→3,6)-*β*-D-Man*p*-(1→	4.91	3.50	3.47	3.6570.90	3.38	3.74
		104.15	65.26	69.13		74.24	73.55

Table 4
Summary of ^{1}H and ^{13}C Chemical Shifts for TLH-3.

	Glycosidic linkage	H1/C1	H2/C2	H3/C3	H4/C4	H5/C5	H6, H'6/C6
A	→4)-α-D-Glc*p*-(1→	5.24	3.46	3.80	3.73	3.78	3.60, 3.71
		102.06	74.36	71.25	75.12	69.13	62.44
B	T-*β*-D-Glc*p*-(1→	4.84	3.67	3.46	4.02	3.57	3.40, 3.49
		100.54	74.78	74.17	71.61	75.22	64.42
Cí	→3,6)-*β*-D-Man*p*-(1→	4.90	3.50	3.47	3.65	3.38	3.74
		104.15	65.26	69.13	70.90	74.24	73.55
Dí	T-*β*-L-*R*ha*p*-(1→	4.92	4.10	3.80	3.61	3.77	1.75
		101.11	71.24	70.61	72.89	69.01	18.19
E	→3,6)-α-D-Glc*p*-(1→	5.07	3.38	3.55	3.41	3.86	3.45
		94.45	72.6	74.4	69.7	72.2	71.1
F	→3)-*β*-D-Gal*p*-(1→	4.37	3.28	3.42	3.93	3.75	3.86
		104.51	72.30	75.26	63.3	71.51	75.7

with previous reports (Golovchenko et al., 2012; Kang et al., 2011; Liu, Lu, et al., 2015; Yin et al., 2010; Zha et al., 2015).

There is a special signal at δ 181.19 ppm in the ^{13}C NMR spectrum (Fig. S5b), which could be attributed to the carboxyl carbon of uronic acid. A cross peak at δ 3.50/63.11 ppm was shown in the HMQC spectrum (Fig. S5d), which was assigned to the methyl group of uronic acid. These results were consistent with the literature data (Yin et al., 2010).

To deduce the sequence of glucosyl residues of TLH-3, the HMBC spectrum was present in Fig. S5e. H-1 of 1,4-linked α-D-Glc*p* (A) have a strong correlation with C-4 of itself and C-3 of 1,3,6-linked α-D-Glc*p* (E). H-1 of 1,3,6-linked α-D-Glc*p* (E) correlated with C-3 of itself, C-4 of 1,4-linked α-D-Glc*p* (A) and C-6 of 1,3,6-linked *β*-D-Man*p* (Cí). H-1 of 1,3,6-linked α-D-Man*p* (Cí) correlated with C-3 of 1,3-linked *β*-D-Gal*p* (F). H-1 of T-*β*-D-Glc*p* (B) correlated with C-6 of 1,3,6-linked *β*-D-Man*p* (Cí). It was also observed that H-1 of 1,3-linked *β*-D-Gal*p* (F), T-α-L-*R*ha*p* (Dí) and T-*β*-D-Glc*p* (B) correlated with C-6 of 1,3,6-linked α-D-Glc*p* (E). Reversely, the cross peaks of C-1 of residues A-F correlated with the corresponding hydrogen were observed in the HMBC spectrum.

4. Discussions

Edible fungi are popular on account of the abundance of functional components and corresponding health benefits. It has been suggested that polysaccharides from mushrooms are the most likely candidates for various biological applications (Li et al., 2006; Li et al., 2011; Mau, Chao, & Wu, 2001). As we all know, effects of mushrooms on alleviating oxidative stress are of great importance for our organism in daily diet. Herein, the antioxidant activities of polysaccharides TLH-1, TLH-2 and TLH-3, which were isolated from the fruiting body of *Tricholoma lobayense*, were evaluated by DPPH, superoxide, hydroxyl and ABTS radicals scavenging assays. The results showed that the antioxidant abilities of TLH-1 and TLH-2 were similar and the maximum effect was about 40% with the tested concentration. However, TLH-3 exhibited the same outstanding activities on scavenging radicals as ascorbic acid, and the activities were about one time more than those of TLH-1 and TLH-2. To explain these differences, structural characterization of the three polysaccharides were determined and the structure-activity relationship was disclosed.

First of all, the antioxidant activities of polysaccharides were closely related to their molecular weights. TLH-1 and TLH-2 with higher molecular weights possessed moderate antioxidant activities, while smaller polysaccharide TLH-3 displayed much stronger radical scavenging abilities, which was in agreement with the report that the polysaccharide with lower molecular weight showed better antioxidant and antitumor activities (Jing, Mao, Geng, & Xu, 2013).

Another pronounced structural difference among the three polysaccharides was the type of linkage. Monosaccharide composition analysis demonstrated that the polysaccharide TLH-1 and TLH-2 mainly consisted of glucose, but TLH-3 was a mixture of glucose and galactose. Methylated analysis demonstrated that TLH-1 and TLH-2 were mostly composed of 1,4-linked α-D-Glc*p*, and TLH-3 was mainly made up of 1,3,6-linked α-D-Glc*p* and 1,3-linked *β*-D-Gal*p*. The glycoside bonds of TLH-1 and TLH-2 were similar and simple, whereas the connection sequence of TLH-3 was very complicated. This was the second reason why the antioxidant activity of TLH-3 was the strongest.

Thirdly, it is also generally believed that branches are important for antioxidant activity of polysaccharides (Volman et al., 2010). The DB value of TLH-3 was almost three times more than that of TLH-1 and TLH-2. GC–MS analysis of methylated polysaccharides showed that TLH-1 and TLH-2 have only one branch point, whereas TLH-3 had two branch points. The branch points of TLH-1 and TLH-2 were 1,3,6-linked α-D-Man*p* and 1,3,6-linked *β*-D-Man*p*, respectively, while the branch points of TLH-3 were 1,3,6-linked α-D-Glc*p* and 1,3,6-linked *β*-D-Man*p*. The high degree of branching was also account for the outstanding activity of TLH-3.

It is well known that the activity of the polysaccharide largely depends on its structure and the influencing factors might be molecular weight, degree of branching, linkage type, monosaccharide composition or glycosidic bonds. As shown in Table 5, some polysaccharides from different mushrooms show decent antioxidant activities because they possess several structural characters listed above. Interestingly, TLH-3 from *Tricholoma lobayense* owns all of the above-mentioned factors, such as low molecular weight, high degree of branching, connections in different ways, favorable linkage type and high contents of galactose, which contribute together to the predominant antioxidant activity.

Table 5
Comparison of antioxidant activity and structural factors of polysaccharides from different mushrooms.

Polysaccharide	IC_{50}(μg/mL)		Structural factors	Reference
	DPPH	Hydroxyl		
CMPA90-1 from *Cordyceps militaris*	>1600	>1600	1, 3-linked α-D-galactose backbone with three branches	Jing et al., 2015
CMP-1 from *Cordyceps militaris*	1150	650	Low molecular weight, composed of 1,4-linked α-D-Glc*p*, 1,6-linked *β*-D-Glc*p* and 1,4-linked *β*-D-Glc*p*	Jing et al., 2014
RVLWP/RVLAP from *Russula vinosa*	1550/3370	–	Backbone composed of glucose and galactose	Liu et al., 2014
Fr-II from *Pleurotus eryngii*	~2500	~3500	Low molecular weight, composed of galactose and mannose	Jing et al., 2013
TAPB1 from *Tremella aurantialba*	–	1770	1,3-linked α-D-Man*p* backbone with two branches	Du et al., 2015
FGM from *Tylopilus ballouii*	–	1600	Fucogalactomannan consisted primarily of mannose and galactose	Lima et al., 2016
FMPS from floral mushroom	~2000	>2000	1,3-linked *β*-D-Glc*p* backbone with one branch	Wang et al., 2015
TLH-1 and TLH-2 from *Tricholoma lobayense*	>500	>500	1,4-linked α-D-Glc*p* backbone with one branch	This work
TLH-3 from *Tricholoma lobayense*	63.1	151.0	Low molecular weight, hyper-branched glucogalactan composed of 1,3,6-linked α-D-Glc*p*, 1,4-linked α-D-Glc*p*, 1,3-linked *β*-D-Gal*p*, 1,3,6-linked *β*-D-Man*p*	This work

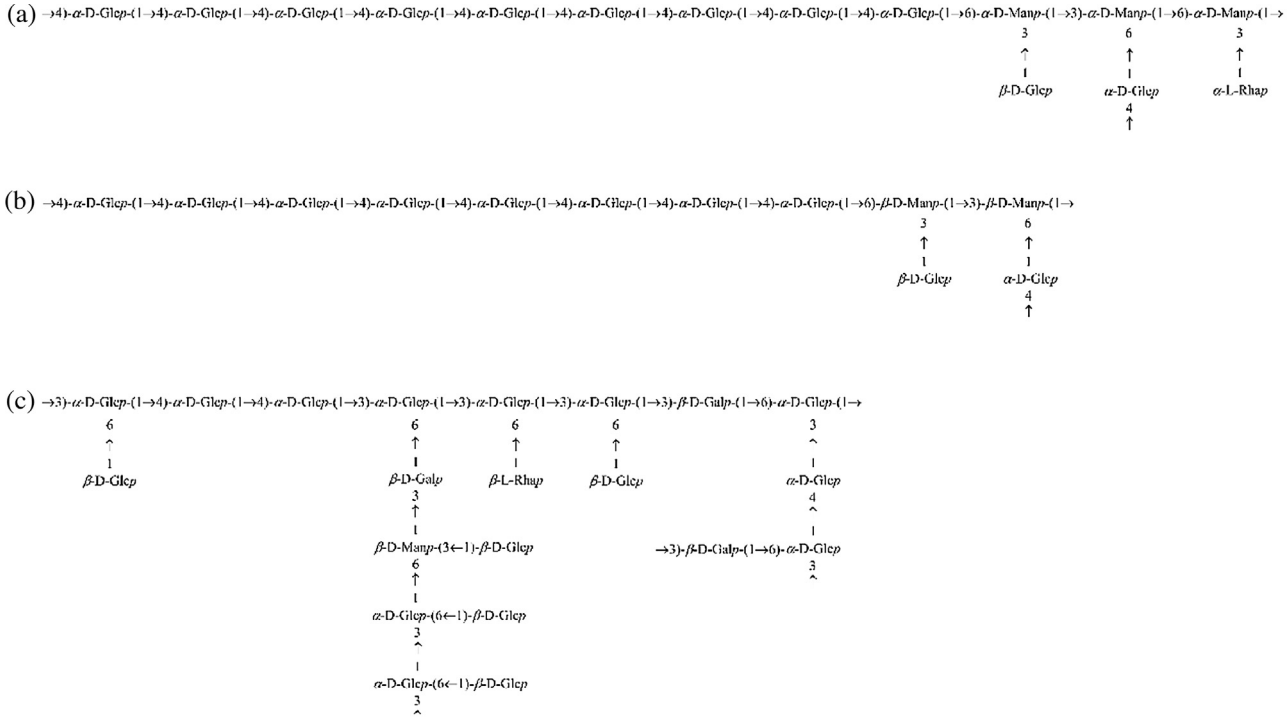

Fig. 3. Possible structures of the repeating units in polysaccharides TLH-1(a), TLH-2(b) and TLH-3(c).

5. Conclusions

In summary, three polysaccharides with purity greater than 99% were obtained from *Tricholoma lobayense.* TLH-1 and TLH-2 were determined to be glucans, whereas TLH-3 is a novel glucogalactan. Based on the structural elucidation, possible structural schemes for TLH-1, TLH-2 and TLH-3 are depicted in Fig. 3. Although the molecular weight of TLH-3 is the lowest, its structure is the most complex. This novel glucogalactan with hyper branch and diverse connection sequence exhibits the most excellent antioxidant activities. Altogether, glucogalactan TLH-3 might be the active substance responsible for the health benefits of the edible mushroom *Tricholoma lobayense*. These results lay the foundation for future research on polysaccharides from *Tricholoma lobayense*.

Acknowledgments

This work was supported by the National Natural Science Foundation of China (31271817, 21301165), the Key Project of Science and Technology of Anhui Province (1501031099) and Doctoral Sci-

entific Research Foundation of Anhui University. The authors thank the testing center of University of Science and Technology of China and Hefei University of Technology for NMR measurements.

Appendix A. Supplementary data

Supplementary data associated with this article can be found, in the online version, at http://dx.doi.org/10.1016/j.carbpol.2016.10.011.

References

Bao, X.-F., Wang, X.-S., Dong, Q., Fang, J.-N., & Li, X.-Y. (2002). Structural features of immunologically active polysaccharides from *Ganoderma lucidum*. *Phytochemistry*, *59*, 175–181.

Barahona, T., Chandía, N. P., Encinas, M. V., Matsuhiro, B., & Zúñiga, E. A. (2011). Antioxidant capacity of sulfated polysaccharides from seaweeds. A kinetic approach. *Food Hydrocolloids*, *25*, 529–535.

Blumenkrantz, N., & Asboe-Hansen, G. (1973). New method for quantitative determination of uronic acids. *Analytical Biochemistry*, *54*, 484–489.

Bradford, M. M. (1976). A rapid and sensitive method for the quantitation of microgram quantities of protein utilizing the principle of protein-dye binding. *Analytical Biochemistry*, *72*, 248–254.

Calonje, M., García Mendoza, C., & Novaes-Ledieu, M. (1996). New contributions to the wall polysaccharide structure of vegetative mycelium and fruit body cell walls of Agaricus bisporus. *Microbiologia (Madrid, Spain)*, *12*, 599–606.

Cao, W., Li, X. Q., Liu, L., Wang, M., Fan, H. T., Li, C., et al. (2006). Structural analysis of water-soluble glucans from the root of *Angelica sinensis* (Oliv.) Diels. *Carbohydrate Research*, *341*, 1870–1877.

Chang, S., & Buswell, J. (1996). Mushroom nutriceuticals. *World Journal of Microbiology and Biotechnology*, *12*, 473–476.

Chang, C. J., Lin, C. S., Lu, C. C., Martel, J., Ko, Y. F., Ojcius, D. M., et al. (2015). Ganoderma lucidum reduces obesity in mice by modulating the composition of the gut microbiota. *Nature Communications*, *6*, 7489.

Chen, X., Cao, D., Zhou, L., Jin, H., Dong, Q., Yao, J., et al. (2011). Structure of a polysaccharide from *Gastrodia elata* Bl.: and oligosaccharides prepared thereof with anti-pancreatic cancer cell growth activities. *Carbohydrate Polymers*, *86*, 1300–1305.

Chen, X., Xiao, F., Wang, Y., Fang, J., & Ding, K. (2012). Structure-activity relationship study of WSS25 derivatives with anti-angiogenesis effects. *Glycoconjugate Journal*, *29*, 389–398.

Chen, L., Zhang, B.-B., Chen, J.-L., & Cheung, P. C. K. (2014). Cell wall structure of mushroom sclerotium (*Pleurotus tuber-regium*): Part 2: Fine structure of a novel alkali-soluble hyper-branched cell wall polysaccharide. *Food Hydrocolloids*, *38*, 48–55.

Das, D., Mondal, S., Roy, S. K., Maiti, D., Bhunia, B., Maiti, T. K., et al. (2009). Isolation and characterization of a heteropolysaccharide from the corm of *Amorphophallus campanulatus*. *Carbohydrate Research*, *344*, 2581–2585.

Du, X., Zhang, Y., Mu, H., Lv, Z., Yang, Y., & Zhang, J. (2015). Structural elucidation and antioxidant activity of a novel polysaccharide (TAPB1) from *Tremella aurantialba*. *Food Hydrocolloids*, *43*, 459–464.

Giavasis, I. (2014). Bioactive fungal polysaccharides as potential functional ingredients in food and nutraceuticals. *Current Opinion in Biotechnology*, *26*, 162–173.

Golovchenko, V. V., Khramova, D. S., Ovodova, R. G., Shashkov, A. S., & Ovodov, Y. S. (2012). Structure of pectic polysaccharides isolated from onion *Allium cepa* L: Using a simulated gastric medium and their effect on intestinal absorption. *Food Chemistry*, *134*, 1813–1822.

Habibi, Y., Heyraud, A., Mahrouz, M., & Vignon, M. R. (2004). Structural features of pectic polysaccharides from the skin of *Opuntia ficus-indica* prickly pear fruits. *Carbohydrate Research*, *339*, 1119–1127.

Liu, J., Wen, X. Y., Kan, J., & Jin, C. H. (2015). Structural characterization of two water-soluble polysaccharides from black soybean (*Glycine max* (L.) Merr.). *Journal of Agricultural and Food Chemistry*, *63*, 225–234.

Jing, X., Mao, D., Geng, L., & Xu, C. (2013). Medium optimization, molecular characterization: And bioactivity of exopolysaccharides from *Pleurotus eryngii*. *Archives of Microbiology*, *195*, 749–757.

Jing, Y., Cui, X., Chen, Z., Huang, L., Song, L., Liu, T., et al. (2014). Elucidation and biological activities of a new polysaccharide from cultured *Cordyceps militaris*. *Carbohydrate Polymers*, *102*, 288–296.

Jing, Y., Zhu, J., Liu, T., Bi, S., Hu, X., Chen, Z., et al. (2015). Structural characterization and biological activities of a novel polysaccharide from cultured *Cordyceps militaris* and its sulfated derivative. *Journal of Agricultural and Food Chemistry*, *63*, 3464–3471.

Kang, J., Cui, S. W., Phillips, G. O., Chen, J., Guo, Q., & Wang, Q. (2011). New studies on gum ghatti (*Anogeissus latifolia*) part II. Structure characterization of an arabinogalactan from the gum by 1D, 2D NMR spectroscopy and methylation analysis. *Food Hydrocolloids*, *25*, 1991–1998.

Kao, P. F., Wang, S. H., Hung, W. T., Liao, Y. H., Lin, C. M., & Yang, W. B. (2012). Structural characterization and antioxidative activity of low-molecular-weights beta-1, 3-glucan from the residue of extracted *Ganoderma lucidum* fruiting bodies. *Journal of Biomedicine and Biotechnology*, *2012*, 673764.

Liu, L., Lu, Y., Li, X., Zhou, L., Yang, D., Wang, L., et al. (2015). A novel process for isolation and purification of the bioactive polysaccharide TLH-3′ from *Tricholoma lobayense*. *Process Biochemistry*, *50*, 1146–1151.

Li, S., Zhang, G., Zeng, Q., Huang, Z., Wang, Y., Dong, T., et al. (2006). Hypoglycemic activity of polysaccharide, with antioxidation: Isolated from cultured *Cordyceps mycelia*. *Phytomedicine*, *13*, 428–433.

Li, H., Xu, J., Liu, Y., Ai, S., Qin, F., Li, Z., et al. (2011). Antioxidant and moisture-retention activities of the polysaccharide from *Nostoc commune*. *Carbohydrate Polymers*, *83*, 1821–1827.

Li, X., Wang, Z., Wang, L., Walid, E., & Zhang, H. (2012). *In vitro* antioxidant and anti-proliferation activities of polysaccharides from various extracts of different mushrooms. *International Journal of Molecular Sciences*, *13*, 5801–5817.

Lima, A. T. M., Santos, M. N., de Souza, L. A. R., Pinheiro, T. S., Paiva, A. A. O., Dore, C. M. P. G., et al. (2016). Chemical characteristics of a heteropolysaccharide from *Tylopilus ballouii* mushroom and its antioxidant and anti-inflammatory activities. *Carbohydrate Polymers*, *144*, 400–409.

Liu, J., & Sun, Y. (2011). Structural analysis of an alkali-extractable and water-soluble polysaccharide (ABP-AW1) from the fruiting bodies of *Agaricus blazei* Murill. *Carbohydrate Polymers*, *86*, 429–432.

Liu, Q., Tian, G., Yan, H., Geng, X., Cao, Q., Wang, H., et al. (2014). Characterization of polysaccharides with antioxidant and hepatoprotective activities from the wild edible mushroom *Russula vinosa* Lindblad. *Journal of Agricultural and Food Chemistry*, *62*, 8858–8866.

Masuko, T., Minami, A., Iwasaki, N., Majima, T., Nishimura, S., & Lee, Y. C. (2005). Carbohydrate analysis by a phenol-sulfuric acid method in microplate format. *Analytical Biochemistry*, *339*, 69–72.

Mau, J.-L., Chao, G.-R., & Wu, K.-T. (2001). Antioxidant properties of methanolic extracts from several ear mushrooms. *Journal of Agricultural and Food Chemistry*, *49*, 5461–5467.

Sun, L., Peng, X., Sun, P., Shi, J., Yuan, X., Zhu, J., et al. (2012). Structural characterization and immunostimulatory activity of a novel linear alpha-(1 → 6)-D-glucan isolated from *Panax ginseng* C. A. Meyer. *Glycoconjugate Journal*, *29*, 357–364.

Villares, A., Mateo-Vivaracho, L., & Guillamón, E. (2012). Structural features and healthy properties of polysaccharides occurring in mushrooms. *Agriculture*, *2*, 452–471.

Volman, J. J., Helsper, J. P., Wei, S., Baars, J. J., van Griensven, L. J., Sonnenberg, A. S., et al. (2010). Effects of mushroom-derived beta-glucan-rich polysaccharide extracts on nitric oxide production by bone marrow-derived macrophages and nuclear factor-kappaB transactivation in Caco-2 reporter cells: Can effects be explained by structure? *Molecular Nutrition & Food Research*, *54*, 268–276.

Wang, L., Zhang, H., Zhang, X., & Chen, Z. (2008). Purification and identification of a novel heteropolysaccharide RBPS2a with anti-complementary activity from defatted rice bran. *Food Chemistry*, *110*, 150–155.

Wang, C., Chen, Y., Hu, M., Ding, J., Xu, C., & Wang, R. (2012). *In vitro* antioxidant activities of the polysaccharides from *Tricholoma lobayense*. *International Journal of Biological Macromolecules*, *50*, 534–539.

Wang, K.-P., Wang, J., Li, Q., Zhang, Q.-L., You, R.-X., Cheng, Y., et al. (2014). Structural differences and conformational characterization of five bioactive polysaccharides from *Lentinus edodes*. *Food Research International*, *62*, 223–232.

Wang, J.-H., Xu, J.-L., Zhang, J.-C., Liu, Y., Sun, H.-J., & Zha, X. (2015). Physicochemical properties and antioxidant activities of polysaccharide from floral mushroom cultivated in Huangshan Mountain. *Carbohydrate Polymers*, *131*, 240–247.

Wasser, S. P. (2002). Medicinal mushrooms as a source of antitumor and immunomodulating polysaccharides. *Applied Microbiology and Biotechnology*, *60*, 258–274.

Weng, B., Lei, J., Jiang, Z., Zhong, Z., Xu, G., & Ye, J. (2013). Substituting wheat bran with Chamaecrista Rotundifolia hay powder in the substrate of *Tricholoma Lobayense* culture: Substrate weight loss dynamics and mass transformation ratios. *Scientia Horticulturae*, *155*, 105–110.

Wu, D. T., Meng, L. Z., Wang, L. Y., Lv, G. P., Cheong, K. L., Hu, D. J., et al. (2014). Chain conformation and immunomodulatory activity of a hyperbranched polysaccharide from *Cordyceps sinensis*. *Carbohydrate Polymers*, *110*, 405–414.

Xu, Y., Dong, Q., Qiu, H., Cong, R., & Ding, K. (2010). Structural characterization of an arabinogalactan from *Platycodon grandiflorum* roots and antiangiogenic activity of its sulfated derivative. *Biomacromolecules*, *11*, 2558–2566.

Xu, S., Xu, X., & Zhang, L. (2012). Branching structure and chain conformation of water-soluble glucan extracted from *Auricularia auricula-judae*. *Journal of Agricultural and Food Chemistry*, *60*, 3498–3506.

Yan, C., Yin, Y., Zhang, D., Yang, W., & Yu, R. (2013). Structural characterization and *in vitro* antitumor activity of a novel polysaccharide from *Taxus yunnanensis*. *Carbohydrate Polymers*, *96*, 389–395.

Yin, Y., Yu, R., Yang, W., Yuan, F., Yan, C., & Song, L. (2010). Structural characterization and anti-tumor activity of a novel heteropolysaccharide isolated from *Taxus yunnanensis*. *Carbohydrate Polymers*, *82*, 543–548.

Zha, X. Q., Xue, L., Zhang, H. L., Asghar, M. N., Pan, L. H., Liu, J., et al. (2015). Molecular mechanism of a new *Laminaria japonica* polysaccharide on the suppression of macrophage foam cell formation via regulating cellular lipid metabolism and suppressing cellular inflammation. *Molecular Nutrition & Food Research*, *59*, 2008–2021.

Zhang, M., Cui, S. W., Cheung, P. C. K., & Wang, Q. (2007). Antitumor polysaccharides from mushrooms: A review on their isolation process:

Structural characteristics and antitumor activity. *Trends in Food Science & Technology*, *18*, 4–19.
Zhao, G., Kan, J., Li, Z., & Chen, Z. (2005). Characterization and immunostimulatory activity of an (1 → 6)-α-D-glucan from the root of *Ipomoea batatas*. *International Immunopharmacology*, *5*, 1436–1445.
Zhu, J., & Wu, M. (2009). Characterization and free radical scavenging activity of rapeseed meal polysaccharides WPS-1 and APS-2. *Journal of Agricultural and Food Chemistry*, *57*, 812–819.
Zhu, W., Han, B., Sun, Y., Wang, Z., & Yang, X. (2012). Immunoregulatory effects of a glucogalactan from the root of *Panax quinquefolium* L. *Carbohydrate Polymers*, *87*, 2725–2729.
Zhu, Q., Jiang, Y., Lin, S., Wen, L., Wu, D., Zhao, M., et al. (2013). Structural identification of (1 → 6)-α-D-glucan, a key responsible for the health benefits of longan, and evaluation of anticancer activity. *Biomacromolecules*, *14*, 1999–2003.